







RESEARCH ARTICLE | JANUARY 06 2025

Double stress overshoot in startup shear flow and failure of Cox–Merz rule of pom-pom polymers

Max G. Schußmann ; Hyeong Yong Song (송형용) ; Kyu Hyun (현 규) ; Manfred Wilhelm ; Valerian Hirschberg  



Physics of Fluids 37, 013109 (2025)

<https://doi.org/10.1063/5.0250133>



View
Online



Export
Citation

Articles You May Be Interested In

Cox–Merz rules from general rigid bead-rod theory

Physics of Fluids (September 2023)

A reexamination of the Cox–Merz rule through the lens of recovery rheology

J. Rheol. (April 2024)

Why the Cox–Merz rule and Gleissle mirror relation work: A quantitative analysis using the Wagner integral framework with a fractional Maxwell kernel

Physics of Fluids (March 2022)



Physics of Fluids

Special Topics Open
for Submissions

[Learn More](#)

Double stress overshoot in startup shear flow and failure of Cox–Merz rule of pom-pom polymers

Cite as: Phys. Fluids **37**, 013109 (2025); doi: [10.1063/5.0250133](https://doi.org/10.1063/5.0250133)

Submitted: 22 November 2024 · Accepted: 9 December 2024 ·

Published Online: 6 January 2025








View Online



Export Citation



CrossMark

Max G. Schußmann,¹  Hyeong Yong Song (송형용),¹  Kyu Hyun (현 규),²  Manfred Wilhelm,¹ 
and Valerian Hirschberg^{1,3,a)} 

AFFILIATIONS

¹Institute for Chemical Technology and Polymer Chemistry, Karlsruhe Institute of Technology (KIT), Engesserstraße 18, 76131 Karlsruhe, Germany

²School of Chemical Engineering, Pusan National University, Busan 46241, Republic of Korea

³Institute for Technical Chemistry, Technical University Clausthal, Arnold-Sommerfeld-Str. 4, 38678 Clausthal-Zellerfeld, Germany

^{a)}Author to whom correspondence should be addressed: valerian.hirschberg@tu-clausthal.de

ABSTRACT

The understanding of long chain branched homopolymer melts in shear flow is of significant interest to polymer science and critical to ensure stable processing. We report on the startup shear flow at a constant shear rate of well-defined pom-pom shaped polymer melts. Pom-poms consist of two stars covalently connected by a single backbone. For low-arm numbers and short arms, a single stress overshoot followed by a steady state is observed, similar to linear and star shaped melts. For one highly branched pom-pom with entangled branches, a double stress overshoot during the startup shear flow could be observed before reaching the steady state viscosity. Additionally, we find that the Cox–Merz rule, which relates the complex viscosity $|\eta^*(\omega)|$ to the steady state shear viscosity $\eta(\dot{\gamma})$, fails at high-shear rates, if the backbone is not self-entangled.

© 2025 Author(s). All article content, except where otherwise noted, is licensed under a Creative Commons Attribution-NonCommercial 4.0 International (CC BY-NC) license (<https://creativecommons.org/licenses/by-nc/4.0/>). <https://doi.org/10.1063/5.0250133>

INTRODUCTION

Introduction to pom-pom

The dynamics of entangled polymers are of fundamental interest to the field of polymer physics and play a crucial role in polymer processing. Since the first useable polyethylene (PE) was discovered in 1933 (high-pressure polymerization),¹ the molecular characterization and flow behavior of its complex branched structure has been the topic of a broad research field.^{2–5} To use simple, constitutive equations, the complex branched structure of low-density polyethylene (LDPE) was simplified in the pom-pom by McLeish and Larson in the late 1990s.⁶ The pom-pom topology contains two star-shaped branching points and a linear chain connecting them as shown in Fig. 1.^{6,7} The pom-pom model by McLeish and Larson is based on the tube model originating from de Gennes⁸ and Doi and Edwards.⁹

Tube model

Tube-based models are an important tool to describe the dynamics of polymer chains.^{8,10–13} The many-body problem of a polymer melt is simplified to a probe chain moving through topological

constraints imposed by surrounding matrix chains. The fundamental concept was introduced by de Gennes, Doi, and Edwards and mainly takes reptation and contour length fluctuation (CLF) into account. To include the influence of the molecular environment of the chain, the tube model was refined through concepts such as double reptation,^{14,15} constraint release (CR), dynamic tube dilution (DTD),¹⁶ and constraint release Rouse motion (CRR).^{17,18} With these additional relaxation mechanisms, the relaxation of long chains is accelerated by the faster relaxation of the short chains compared to their monodisperse environment. Due to the DTD picture, tube models have been improved to near quantitative agreement in SAOS with not only linear but also branched model polymers, such as comb, H-shaped, and pom-pom.^{19–28} After the relaxation of outer parts of the molecules, the relaxed parts act as a solvent toward the inner parts of the chains. The diluting effect results in the remaining unrelaxed chains moving in an effectively dilated tube. For branched chains, the hierarchical relaxation concept is introduced where the most outer chains relax first, and all inner chains are frozen until the outer arms are fully relaxed.¹² Similarly, for branched chains, the relaxed arms act as a solvent around the backbone, reducing its effective entanglements. The effective entanglements are given by

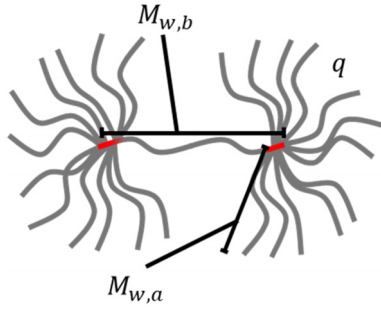


FIG. 1. Schematic of a PS pom-pom: two star-shaped branching points are connected by a linear chain. Red chain part shows branching point as described in experimental section.

$$Z_{b,eff} = \phi_b * Z_b, \quad (1)$$

where ϕ_b is the backbone volume fraction and Z_b is the undiluted backbone entanglements from the backbone molecular weight $Z_b = M_{w,b}/M_e$.

Cox-Merz rule

The Cox–Merz rule relates the magnitude of the complex viscosity $|\eta^*(\omega)|$ at a given angular frequency ω in the linear regime being equal to the nonlinear steady-state shear viscosity $\eta(\dot{\gamma})$ at a corresponding shear rate $\dot{\gamma}$.²⁹

$$|\eta^*(\omega)| = \eta(\dot{\gamma})|_{\dot{\gamma}=\omega}. \quad (2)$$

Despite being derived from empirical observation and its simplicity, there are a vast amount of examples where the Cox–Merz rule holds true.^{13,30–33} However, deviations between the viscosity obtained from steady shear and oscillatory shear and therefore failure of the Cox–Merz rule also has been observed, especially for highly branched, well-defined architectures.³⁴

Previous works

The investigation of startup shear flow is of relevance due to its occurrence during both extrusion and injection molding.³⁵ Although experimental rheological data on pom-poms is very rare, some pom-pom systems have been studied under linear, small amplitude

oscillatory shear flow (SAOS).^{36–39} Only recently, efforts were made to investigate the nonlinear behavior in extension and shear flow.^{40–46} From these studies, it became clear that the ratio of chain lengths of backbone and arms, and consequently, the resulting relaxation times is a critical molecular characteristic needed for the prediction of their flow properties. Therefore, molecular topology controls linear and nonlinear properties in shear and elongation in homopolymer melts. During startup shear flow of most polymeric samples, a typical stress overshoot can be observed before the steady state viscosity is reached.^{7,41,47–52}

More than a single stress overshoot was only found for two samples, one made of a highly branched comb and one of a bidisperse linear melt. For the comb, Snijders *et al.* could observe two stress overshoots in startup behavior in simple shear. The two overshoots were attributed to arm orientation (first overshoot) and backbone stretch and orientation (second overshoot).⁴⁰ For the bidisperse blend, similarly, two overshoots could be detected relating to the orientation of the short and stretch of the longer chains.^{53,54}

Herein, we investigate seven different pom-pom shaped polymers with arm molecular weight $M_{w,a} = 9\text{--}40 \text{ kg mol}^{-1}$, backbone molecular weight $M_{w,b} = 100 \text{ or } 220 \text{ kg mol}^{-1}$, and arm number $q = 5\text{--}22$ in nonlinear startup shear flow due to their different effective backbone entanglements and variety of arm and backbone relaxation time combinations. The data are analyzed to understand the molecular origin of the shear stress growth coefficient and to test the validity of the Cox–Merz rule for highly branched polymer systems.

Experiment

The synthesis of the herein investigated pom-poms was described in detail in previous works, together with in-depth molecular and SAOS characterization.^{42,43,55,56} In short, an isoprene-styrene-isoprene triblock copolymer backbone (mol ratio of PS to PI $\gg 10:1$) was synthesized with a short (typically 50 monomers) isoprene end block acting as a functional end group. The polyisoprene blocks were epoxidized using hydrogen peroxide and formic acid. In the third step, the arms were polymerized separately and subsequently grafted onto the epoxidized backbone ends. The molecular parameters of the pom-poms are listed in Table I, and an overview of the entanglement classification is given in Table II. The general nomenclature within this article is $M_{w,b} - 2x \ q - M_{w,a}$, where molecular weight is given in kg mol^{-1} . Backbones are considered as self-entangled if a discrete rubber plateau is visible with a phase angle δ below 45° .

TABLE I. Molecular parameters of the PS pom-pom, denoted as follows: $M_{w,b} - 2x \ q - M_{w,a}$. $M_{w,b}$ is the molecular weight of the arms, q is the number of arms per star/pom, and $M_{w,a}$ is the molecular weight of the backbone. The dispersity of the backbone, arms, and total pom-pom are \mathcal{D}_b , \mathcal{D}_a , and \mathcal{D}_t , respectively. The number of entanglements of the backbone Z_b and the sidechains Z_a is calculated using an entanglement molecular weight of $M_e = 16.8 \text{ kg mol}^{-1}$.⁴² ϕ_b is the volume fraction of the backbone.

Sample	$M_{w,b} \text{ (kg mol}^{-1}\text{)}$	Z_b	\mathcal{D}_b	$M_{w,a} \text{ (kg mol}^{-1}\text{)}$	Z_a	\mathcal{D}_a	q	ϕ_b	\mathcal{D}_t	$Z_{b,eff}$
100k-2 \times 11-9k	100	5.95	1.05	9	0.54	1.02	11	0.34	1.13	2.00
100k-2 \times 5-25k	100	5.95	1.05	25	1.49	1.05	5	0.29	1.12	1.70
100k-2 \times 12-24k	100	5.95	1.05	24	1.43	1.05	12	0.15	1.18	0.88
100k-2 \times 22-25k	100	5.95	1.05	25	1.49	1.14	22	0.08	1.15	0.50
100k-2 \times 12-40k	100	5.95	1.05	40	2.38	1.08	12	0.09	1.16	0.56
220k-2 \times 12-25k	220	13.1	1.06	25	1.49	1.08	12	0.27	1.08	3.51
220k-2 \times 10-40k	220	13.1	1.06	40	2.38	1.10	10	0.22	1.09	2.82

TABLE II. Overview of the entanglements of arm and backbone and arm numbers ($\delta < 45^\circ$). N=No, Y=Yes. Categories are assigned based on the small amplitude oscillatory shear behavior.

Sample	Backbone self-entangled	Arm entangled	Category
100k-2 \times 11-9k	Y	N	1
100k-2 \times 5-25k	N	Y	2
100k-2 \times 12-24k	N	Y	2
100k-2 \times 22-25k	N	Y	2
100k-2 \times 12-40k	N	Y	2
220k-2 \times 12-25k	Y	Y	3
220k-2 \times 10-40k	Y	Y	3

All rheological measurements were conducted on a TA Instruments ARES G2 rheometer under nitrogen inert gas atmosphere. For small amplitude oscillatory shear experiments, a 13 mm parallel plate geometry was used. Frequency sweeps typically between 0.01 and 100 rad s⁻¹ were conducted in the linear regime, which was determined beforehand by strain sweeps at 100 rad s⁻¹. Strain amplitudes between 0.1% and 5% were used for the frequency sweeps at temperatures between 125 and 220 °C. For stress growth experiments, a home-built cone-partitioned plate geometry (CPP) according to Costanzo *et al.*⁵⁷ with 10 mm inner diameter and 25 mm cone with 0.1 rad was used in a temperature range between $T = 160$ – 180 °C and shear rates between $\dot{\gamma} = 0.001$ – 1 s⁻¹ typically, for some samples up to $\dot{\gamma} = 30$ s⁻¹. Data were shifted to the reference temperature using the shift factors from the small amplitude oscillatory shear mastercurve. To ensure data integrity and avoid measurement instabilities which simple shear is prone to, selected shear rates were repeated multiple times. Correct sample loading onto the CPP was ensured by comparing frequency sweeps to parallel plate measurements before startup shear measurements and between successive startup tests to detect possible edge fracture artifacts according to established procedures.⁵⁸ Furthermore data were compared between different sample loadings to ensure reproducibility. The relaxation time τ_l is taking from the inverse of the crossover

frequency to the terminal regime and used to calculate the Wi number. A Maxwell mode was fitted to G' and the crossover of the Maxwell mode was used if the pom-pom showed Rouse relaxation before the terminal regime. Earlier works on the pom-poms in extensional flow revealed that $\tau_l \sim \tau_s$, with τ_s being the stretch relaxation time.⁴⁵ The orientation relaxation time τ_b is longer than τ_s , as also predicted by the pom-pom model.⁶

RESULTS AND DISCUSSION

Small amplitude oscillatory shear experiments

The small oscillatory shear response of the pom-pom samples has been reported and discussed in detail in previous works.^{42,43,45} The samples can be divided into three main categories and examples are shown in Fig. 2(a). Category 1 is represented by 100k-2 \times 11-9k. The sample shows a small Rouse regime at high frequencies due to the unentangled arms, followed by a rubber plateau due to the self-entangled backbone, and a terminal regime identified by the slopes of $G' \propto \omega^2$ and $G'' \propto \omega^1$. Category 2 is represented by the samples 100k-2 \times 5-25k, 100k-2 \times 12-24k, 100k-2 \times 22-25k, and 100k-2 \times 12-40k and shows three distinct relaxation regimes: at low frequencies, the terminal regime is found; at medium frequencies, a Rouse relaxation regime can be identified where G' and G'' increase in parallel; and at high frequencies, a rubber plateau is found where $G' > G''$. The high-frequency rubber plateau is a result of the longer arms compared to Category 1 and caused by arm and backbone entanglement effects, while the Rouse relaxation behavior reveals a not self-entangled backbone caused by dynamic dilution of the backbone in the arms. The samples 220k-2 \times 12-25k and 220k-2 \times 10-40k belong to category 3 and show two rubber plateaus, due to their self-entangled backbone, as well as a terminal regime. In Fig. 2(b), the van Gurp–Palmen plot (δ vs $|G^*|$) is shown. The two different relaxation times of the arm and the backbone can be identified clearly for all samples.

To investigate the dilution of the backbone in the arms, the value of the phase angle minimum of the backbone $\delta_{b,min}$ as a function of the effective backbone entanglements $Z_{b,eff} = \phi_b * Z_b$ is shown in Fig. 3. Pom-poms from Table II and from the literature^{37,39,59} are shown together with the literature data on combs.^{20,60–63} If the phase

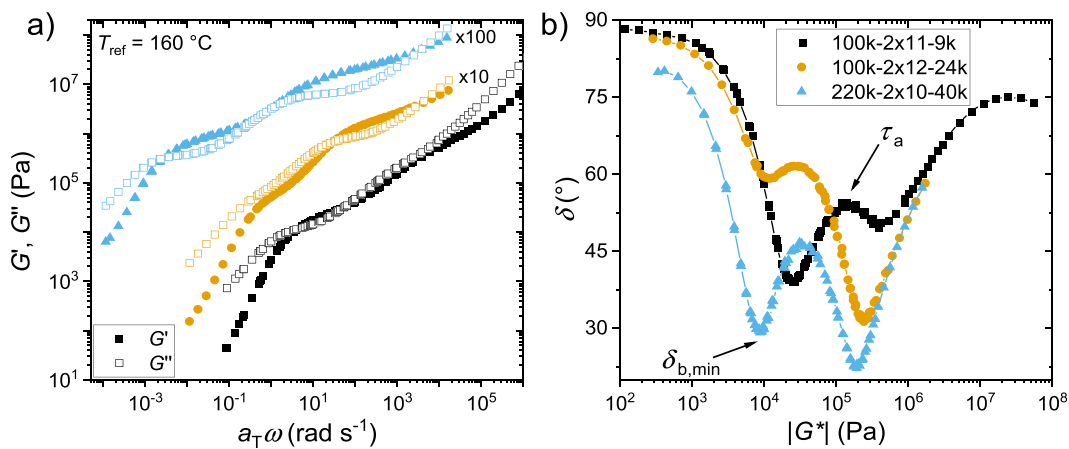


FIG. 2. (a) Mastercurve of pom-poms 100k-2 \times 11-9k, 100k-2 \times 12-24k, and 220k-2 \times 10-40k and (b) their van Gurp–Palmen plot, clearly showing distinct relaxation mechanism for arms and backbone.

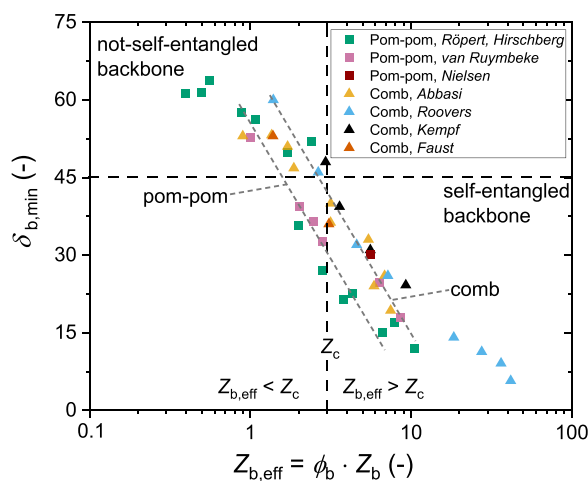


FIG. 3. Phase angle of the backbone minimum shown as a function of effective backbone entanglements. Dashed lines are a guide to the eye.

angle is below 45° , the moduli display a rubber plateau which is caused by entangled backbone chains. For $\delta_{b,min} > 45^\circ$, $G'' > G'$ and therefore showing Rouse-like behavior relating to not self-entangled chains. Two regions can be identified for comb and pom-pom polymers. For $Z_{b,eff} > 3$, the backbone minimum phase angle is found to be below 45° , indicating that the backbone is self-entangled, meaning that the backbone is entangled with other backbones. For $Z_{b,eff} < 3$, the $\delta_{b,min}$ phase angle is found to be above 45° , indicating that the backbone is not self-entangled. These findings agree with the general dynamic dilution theory for linear polymer melts and solutions, where the critical entanglement number $Z_c \sim 3$ is found.⁶⁴ As indicated by the gray dotted guide lines in Fig. 3, the data might suggest that pom-poms are more elastic (lower phase angle) in SAOS than combs. A comb and pom-pom with the same molecular parameters (same $M_{w,b}$, q , $M_{w,a}$) are needed to confirm this.

Startup shear experiments

The LVE and the shear stress growth coefficient η^+ of the pom-poms at selected shear rates are shown as a function of time t in Fig. 4 (pom-pom 100k-2 \times 12-40k shown in Fig. 5). In general, shear thinning can be observed for all shear rates. As shown in Figs. 4(a) and 4(b) for pom-poms with shorter arms or lower arm number, i.e., higher backbone volume fractions, the startup shear behavior is similar to previously reported studies on linear, star, and most comb shaped polymers. The shear stress growth coefficient has a strong overshoot followed by a steady state viscosity. At very low-strain rates, the stress growth coefficient coincides with the zero-shear viscosity obtained from SAOS. At medium shear rates i.e., 0.3 s^{-1} , a weak undershoot can be detected, disappearing at lower and higher shear rates. In Figs. 4(c)–4(f), startup shear behavior for pom-poms with longer arms or higher arm numbers is shown. Similarly, a stress overshoot ($\gamma_{2,pp}$, see Fig. 5) followed by an undershoot and a steady state viscosity can be observed. At high-shear rates, no steady state viscosity is obtained at long times, but the viscosity increases steadily with time, i.e., in (c) at 2.5 s^{-1} . At around 0.5 s and 10^4 Pa s an increase in the transient data above the LVE is measured. This is atypical for polymer melts, as they

show shear thinning in general. The authors suspect that the increase above the LVE might be a result of the compliance of the rheometer transducer and no true material response.

In Fig. 5, σ^+ of 100k-2 \times 12-40k is shown as a function of the applied strain. Two distinct stress overshoots can be observed. They are named according to the strain at which the stress overshoot occurs, and the subscript “pp” is short for pom-pom. The first stress overshoot can be observed for strain rates above $\dot{\gamma} = 1 \text{ s}^{-1}$ with increasing strain, saturating at $\gamma_{1,pp} = 2.3$ for $\dot{\gamma} > 4.5 \text{ s}^{-1}$. As result of tube orientation, σ_{max}^+ occurs at $\gamma = 2.3$ for linear chains.^{48,65} The second stress overshoot can be observed at $\gamma_{2,pp} = 1.3$ for $\dot{\gamma} \geq 0.0135 \text{ s}^{-1}$. With increasing shear rates, $\gamma_{2,pp}$ increases and then saturates at $\gamma_{2,pp} \approx 7$ for shear rates above $\dot{\gamma} = 1 \text{ s}^{-1}$. Measurements at $\dot{\gamma} > 3 \text{ s}^{-1}$ were typically terminated by normal force transducer overload before reaching a steady state. Surprisingly, a third stress maxima can be observed around $\gamma_{3,pp} = 650$. Although measurements were conducted with great care to ensure reliable data, one cannot exclude a measurement artifact at so large strains.

To further investigate the second stress overshoot and its molecular origin, $\gamma_{2,pp}$ is shown as a function of Wi in Fig. 6(a) for different $M_{w,b}$, $M_{w,a}$, and q . The gray dotted line displays the prediction of the Doi-Edwards tube model. For linear chains and $Wi < 1$, a constant strain of $\gamma = 2.3$ is found, while for $Wi > 1$, a weak strain rate dependency on $\gamma_{2,pp}$ is obtained ($\gamma_{2,pp} \sim Wi^{1/3}$, gray dashed line).⁶⁵ For the pom-pom samples at $Wi < 20$, a weak strain rate dependency of $\gamma_{2,pp} \sim Wi^{1/2}$ can be observed. However, the lower threshold of $\gamma_{2,pp}$ is not $\gamma_{2,pp} = 2.3$ as predicted by the DE model and observed experimentally for linear chains⁶⁶ but decreases to $\gamma_{2,pp} \approx 1$. For the sample 100k-2 \times 12-40k, $\gamma_{2,pp}$ reaches a plateau strain of $\gamma_{2,pp} \sim 7$ for $Wi > 20$. For linear chains, no γ plateau at high Wi was observed in the literature and only Snijkers *et al.* reported a $\gamma_{2,pp}$ plateau for a comb backbone.^{40,67–69} As shown in Fig. 6(a) by the vertical, orange dashed line, $\gamma_{2,pp}$ at $Wi = 1$ increases with decreasing arm molecular weight. For the arm molecular weight range investigated here, we find a linear decrease in the stress overshoot strain as a function of arm molecular weight in kg mol^{-1} with a slope of -0.073 as shown in Fig. 6(b). Under shear, the macroscopic strain induces a microscopic orientation of the chains. The backbone end-to-end vector \vec{r}_b is rotated into the flow direction, as shown by Brownian molecular dynamics simulation for pom-pom, H-shaped and linear chains.^{67,70–72} If the arm length is increased, the relaxation of the star shaped branched point is slowed down, independent of the arm number.^{21,73} Therefore, movement of the two branch points at each end of the backbone is also reduced. As a result, the macroscopic strain to reach the same microscopic orientation of \vec{r}_b might be reduced with increased arm molecular weight.

The different γ_1 and γ_2 of the pom-pom and comb are further analyzed in Fig. 7 as a function of Wi for the herein reported pom-pom sample 100k-2 \times 12-40k as well as the previously reported data on the comb sample C642 (275k-29-47k, “Roover Comb”).⁴⁰ The arm relaxation times of the pom-pom and comb are $\tau_{a,pp}$ and $\tau_{a,c}$, respectively. Both are determined from the local maximum of the phase angle. For comb and pom-pom, the strain of the stress overshoot increases with increasing shear rate before saturating at a constant value. A power law exponent of 0.5 for γ_1 and γ_2 as a function of Wi can be observed for their respective low-shear rates. While the two overshoots of the comb can be observed at $\gamma_{1,c} \approx 2$ and $\gamma_{2,c} \approx 12$, the pom-pom exhibits its overshoots at $\gamma_{1,pp} \approx 2$ and $\gamma_{2,pp} \approx 7$. The different strains of γ_2 could be a result of the different backbone lengths of

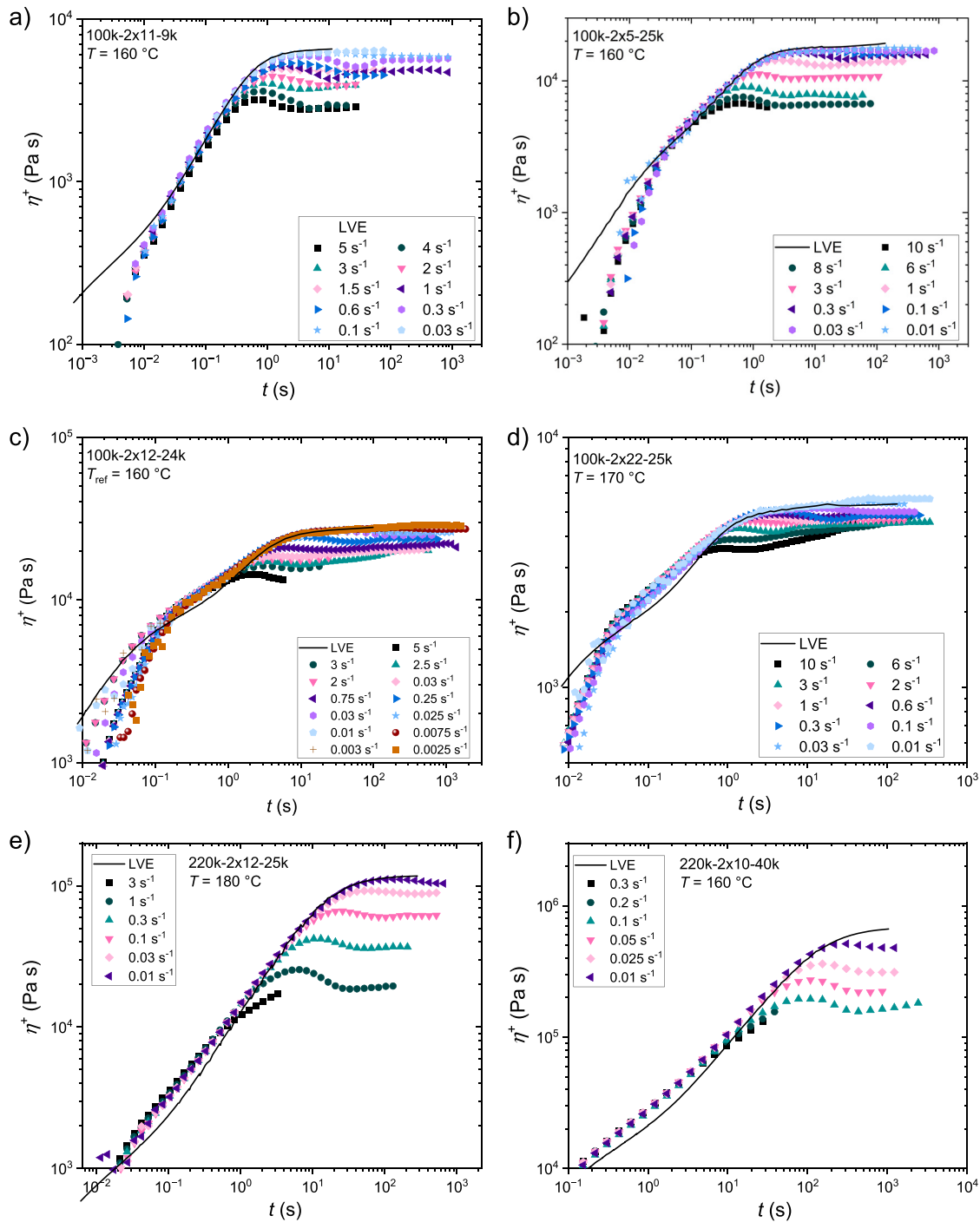


FIG. 4. Shear stress growth coefficient is shown as a function of time at selected shear rates for pom-pom (a) 100k-2 × 11-9k, (b) 100k-2 × 5-25k, (c) 100k-2 × 12-24k, (d) 100k-2 × 22-25k, (e) 220k-2 × 12-25k, and (f) 220k-2 × 10-40k. For higher shear rates, the viscosity measurement is terminated by the normal force exceeding the transducer capacity, i.e., $\dot{\gamma} = 3 \text{ s}^{-1}$ and $\dot{\gamma} = 5 \text{ s}^{-1}$ in (c) or 3 s^{-1} in (e).

the two samples but indicating only a very weak $M_{w,b}$ dependency of γ_2 . Investigations of the pom-poms in extensional flow revealed that τ_l is close to the stretch relaxation time τ_s .⁴⁵ In the steady shear experiment the strain of the overshoot is constant for chain orientation and

increases if chain stretch contributes. In Fig. 7, $\gamma_{2,pp}$ is constant at $Wi < 1$ and increases for $Wi > 1$, therefore suggesting a backbone stretch contribution to γ_2 for $Wi > 1$, supporting the findings from uniaxial elongational flow that for pom-poms $\tau_l \sim \tau_s$. For both

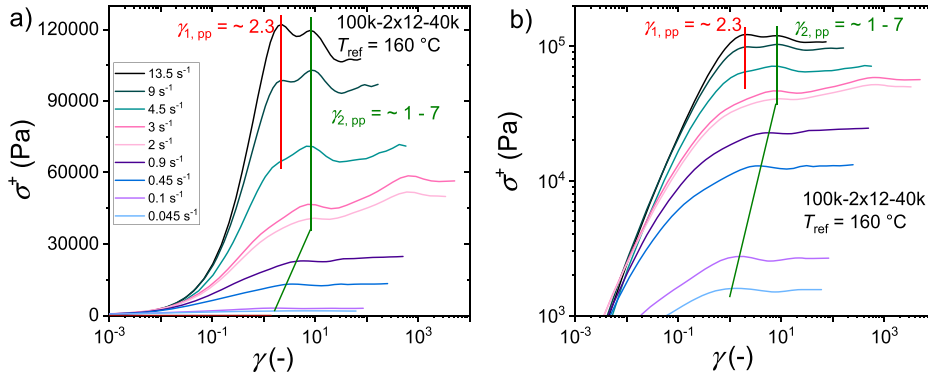


FIG. 5. Shear stress growth function in (a) linear and (b) logarithmic scaling shown as a function of applied strain for selected strain rates between 0.00135 and 13.5 s⁻¹.

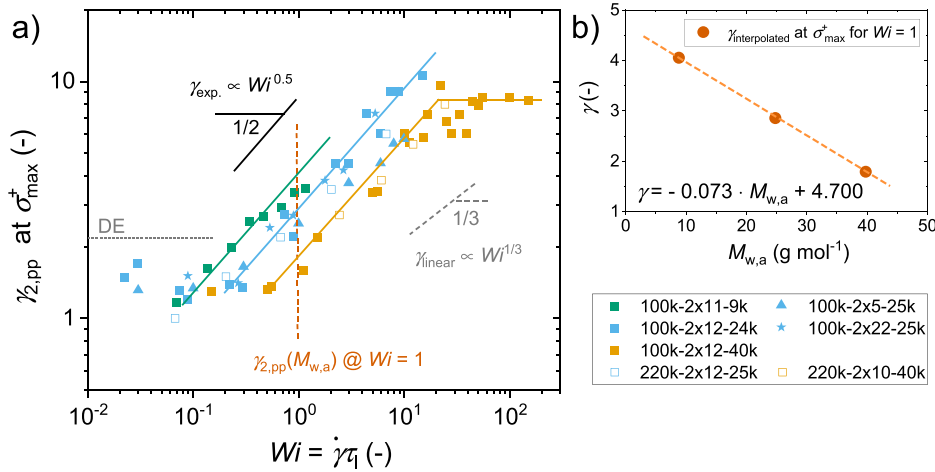


FIG. 6. (a) Strain of the second stress overshoot $\gamma_{2,pp}$ shown as a function of the Weissenberg number for pom-pom shaped samples with different $M_{w,b}$, $M_{w,a}$, and q . (b) Interpolated strain $\gamma_{2,pp}$ shown as a function of $M_{w,a}$ of all samples of (a).

pom-pom and comb, γ_1 can be observed for strain rates faster than the arm relaxation time. Since $\gamma_1 \sim 2$, this suggests arm orientation as a molecular origin, as stress overshoots due to chain orientation occur at $\gamma \sim 2$ as shown previously for linear chains.⁶⁶

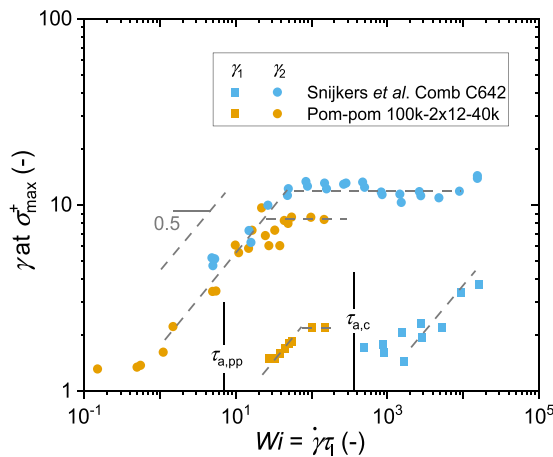


FIG. 7. Strain of the stress overshoots shown as a function of the Weissenberg number for sample 100k-2 × 12-40k and the comb C642 (275k-29-47k) investigated by Snijkers *et al.*⁴⁰

We attribute the two stress overshoots found for the pom-pom topology and their origin as follows: the first stress overshoot is a result of the arm orientation due to the occurrence at $\dot{\gamma} > 1/\tau_a$ and the strain of $\gamma_1 \sim 2$. The second stress overshoot is attributed to backbone orientation and stretch at higher shear rates. This interpretation of the data are in line with previous works on comb and linear samples.^{40,53,54} A double stress overshoot in startup shear was previously reported by Snijkers *et al.*⁴⁰ and only observed for one comb sample. Solutions of bimodal linear polymers investigated by Osaki *et al.*⁵⁴ also showed a double stress overshoot for only one sample among many. All three systems, which show the double stress overshoots, have similar short chain molecular weights (40k, 40k, and 47k), similar long chain volume fractions $\phi_L \sim 0.1$ and well-separated relaxation times of the long and short chain. The mastercurves are similar in their overall shape, consisting of a high-frequency rubber plateau followed by a Rouse and terminal regime at lower frequencies.

Evaluation of Cox-Merz rule

In startup shear measurements, after the stress exhibits one or more maxima, a steady state viscosity is reached at large strains, as shown in Fig. 4(a). In Fig. 8, the normalized steady state viscosity is shown as a function of Wi for (a) pom-poms with $M_{w,b} = 100$ kg mol⁻¹, $M_{w,a} = 25$ kg mol⁻¹ and increasing q (5, 12, and 22) and (b) $M_{w,b} = 100$ kg mol⁻¹, $q \sim 12$ and increasing $M_{w,a}$ (9, 24, and

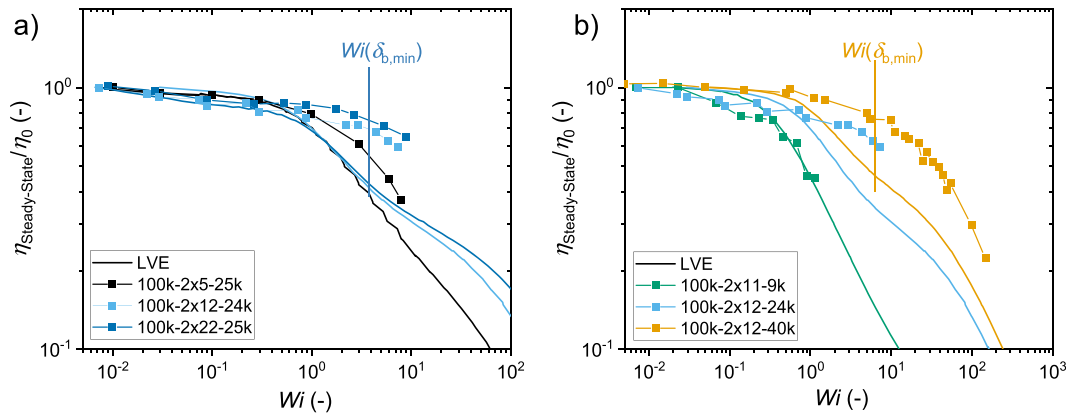


FIG. 8. Steady state viscosity obtained from stress growth experiments normalized to the zero-shear viscosity is shown as a function of the Weissenberg number for (a) increasing arm number and (b) increasing arm molecular weight.

40 kg mol⁻¹). At $Wi > 1$, a deviation of $|\eta^*(\omega)| < \eta(\dot{\gamma})$ can be observed. The deviation between $|\eta^*(\omega)|$ and $\eta(\dot{\gamma})$ is the largest around the backbone phase angle minimum $Wi(\delta_{b,min})$ of up to 40%. Overall, the deviation between the steady state viscosity (startup) and the absolute value of the complex viscosity (SAOS) increases with increasing arm number and length, i.e., reduced backbone volume fraction.

The validity or failure of the Cox–Merz rule should depend on the molecular parameters. The failure typically occurs at frequencies where only the backbone is not yet relaxed and is showing Rouse relaxation. Therefore, we investigate the validity or failure of the Cox–Merz rule as a function of the $Z_{b,eff}$. The steady state viscosity $\eta(\dot{\gamma})$ is increased compared to the complex viscosity from SAOS with the maximum deviation around $Wi(\delta_{b,min})$ as illustrated in Fig. 9(a). The deviation at $Wi(\delta_{b,min})$ is shown as a function of $Z_{b,eff}$ in Fig. 9(b) for the herein investigated pom-poms and the literature data on combs. Two distinct areas can be identified depending on $Z_{b,eff}$. For $Z_{b,eff} < 3$, the deviation from the Cox–Merz rule increases with decreasing $Z_{b,eff}$. For $Z_{b,eff} > 3$, the Cox–Merz rule is fulfilled at all Wi numbers investigated, showing that $Z_{b,eff}$ is the critical molecular criteria for the validity and failure of the Cox–Merz rule. Similar results were previously

reported for combs, with a deviation from the Cox–Merz rule at higher shear rates, which was correlated with their low $Z_{b,eff}$.³⁴ While deviations from the Cox–Merz rule have been observed before, they are fairly uncommon in monodisperse homopolymer melts. The literature data and our data suggest that the deviations can only be observed for systems with low-effective backbone entanglements as a result of high-branching density.³⁴ For unentangled polymer solutions, deviations from the Cox–Merz rule have been observed as well.⁶⁶

Surprisingly, the herein found difference between the startup shear measurements and the LVE obtained from SAOS was not observed in earlier works on elongational flow.^{42,45} When the LVE is compared to the extensional viscosity at strains smaller than the occurrence of extensional hardening or thinning, the same viscosity is measured in extension and in SAOS.

CONCLUSION

We present experimental, nonlinear startup shear investigations of well defined, low-disperse polystyrene pom-pom polymers. We find that the strain of the main (second) stress overshoot is a function of the arm molecular weight of the pom-pom, but independent of the

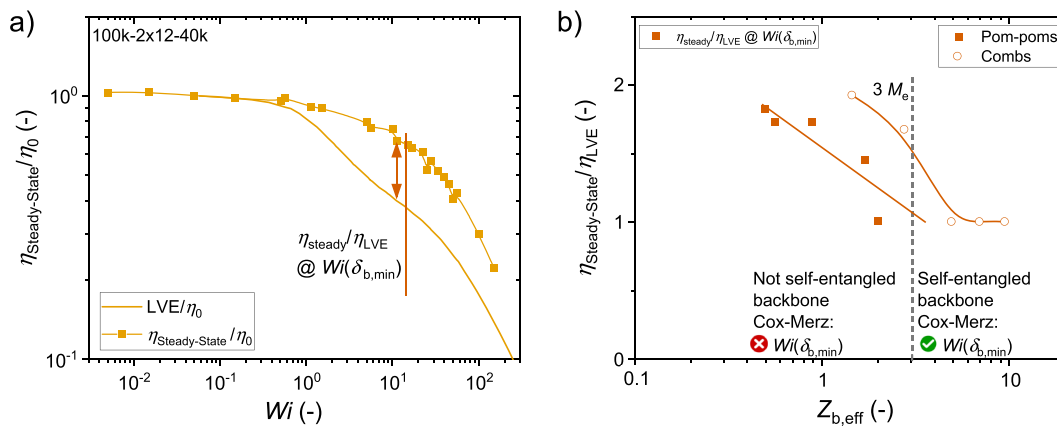


FIG. 9. (a) Determination of the deviation between the steady state shear viscosity and the LVE. (b) Deviation shown as a function of the effective backbone entanglements for pom-poms (this work) and combs.³⁴ Lines are a guide to the eye.

backbone molecular weight and the arm number ($q \geq 5$). For the pom-pom $100k-2 \times 12-40k$, a double stress overshoot of a pom-pom topology could be observed for the first time. When comparing startup data of a comb polymer with the data on pom-poms, similarities, and differences emerge. For pom-poms and combs, the first stress overshoot can be attributed to the arms and occurs at the same strain ($\gamma_{1,c,p} \approx 2$). The second stress overshoot increases with shear rate and saturates at high-strains rates at different strains for the pom-pom ($\gamma_{2,pp} \approx 7$) and the comb ($\gamma_{2,c} \approx 12$). The investigation of the pom-poms additionally reveals a strong deviation (up to $>40\%$) from the commonly used Cox–Merz rule for homopolymer melts $|\eta^*(\omega)| = \eta(\dot{\gamma})|_{\dot{\gamma}=\omega}$ at effective backbone entanglements $Z_{b,eff} < 3$ and high-branching numbers. Review of the literature data reveals similar results for combs.

ACKNOWLEDGMENTS

M.G.S. thanks the Karlsruhe House of Young Scientists (KHYS) for financial support. Dr. H.Y.S. thanks the Alexander von Humboldt foundation for a postdoctoral stipend. The authors thank Professor Yuichi Masubuchi for fruitful discussions. Access to the IRIS software by Professor H. Henning Winter is highly appreciated. The authors thank Dr. Michael Pollard for proofreading the manuscript as a native English speaker.

AUTHOR DECLARATIONS

Conflict of Interest

The authors have no conflicts to disclose.

Author Contributions

Max G. Schußmann: Conceptualization (equal); Data curation (equal); Formal analysis (equal); Investigation (equal); Methodology (equal); Visualization (equal); Writing – original draft (equal); Writing – review & editing (equal). **Hyeong Yong Song:** Data curation (supporting); Formal analysis (supporting); Investigation (supporting); Methodology (supporting); Visualization (equal); Writing – original draft (equal); Writing – review & editing (equal). **Kyu Hyun:** Conceptualization (supporting); Data curation (supporting); Formal analysis (supporting); Funding acquisition (supporting); Supervision (supporting); Writing – original draft (supporting); Writing – review & editing (supporting). **Manfred Wilhelm:** Conceptualization (equal); Data curation (equal); Formal analysis (equal); Funding acquisition (equal); Writing – original draft (equal); Writing – review & editing (equal). **Valerian Hirschberg:** Conceptualization (equal); Data curation (equal); Formal analysis (equal); Investigation (equal); Methodology (equal); Writing – original draft (equal); Writing – review & editing (equal).

DATA AVAILABILITY

The data that support the findings of this study are available from the corresponding author upon reasonable request.

REFERENCES

- E. W. Fawcett and R. O. Gibson, United Kingdom Patent GB471590A (1936).
- M. Gahleitner, “Melt rheology of polyolefins,” *Prog. Polym. Sci.* **26**(6), 895–944 (2001).
- H. Münstedt, “Rheological properties and molecular structure of polymer melts,” *Soft Matter* **7**(6), 2273–2283 (2011).
- F. N. Cogswell, *Polymer Melt Rheology* (Woodhead Publishing, 1981).
- J. L. White and D. D. Choi, *Polyolefins: Processing, Structure Development, And Properties* (Hanser Verl., 2004).
- T. C. B. McLeish and R. G. Larson, “Molecular constitutive equations for a class of branched polymers: The pom-pom polymer,” *J. Rheol.* **42**(1), 81–110 (1998).
- N. J. Inkson, T. C. B. McLeish, O. G. Harlen, and D. J. Groves, “Predicting low density polyethylene melt rheology in elongational and shear flows with ‘pom-pom’ constitutive equations,” *J. Rheol.* **43**(4), 873–896 (1999).
- P. G. de Gennes, “Reptation of a polymer chain in the presence of fixed obstacles,” *J. Chem. Phys.* **55**(2), 572–579 (1971).
- M. Doi and S. F. Edwards, “Dynamics of concentrated polymer systems. Part 1.—Brownian motion in the equilibrium state,” *J. Chem. Soc. Faraday Trans. 2 Mol. Chem. Phys.* **74**(0), 1789–1801 (1978).
- M. Doi and S. F. Edwards, *The Theory of Polymer Dynamics*, Reprint (Clarendon Press, Oxford, 2013).
- H. Watanabe, “Viscoelasticity and dynamics of entangled polymers,” *Prog. Polym. Sci.* **24**(9), 1253–1403 (1999).
- T. C. B. McLeish, “Tube theory of entangled polymer dynamics,” *Adv. Phys.* **51**(6), 1379–1527 (2002).
- J. M. Dealy, D. J. Read, and R. G. Larson, *Structure and Rheology of Molten Polymers: From Structure to Flow Behavior and Back Again* (Carl Hanser Verlag, 2018).
- C. Tsenoglou, “Molecular weight polydispersity effects on the viscoelasticity of entangled linear polymers,” *Macromolecules* **24**(8), 1762–1767 (1991).
- J. des Cloizeaux, “Double reptation vs. Simple reptation in polymer melts,” *Europhys. Lett.* **5**(5), 437 (1988).
- G. Marrucci, “Relaxation by reptation and tube enlargement: A model for poly-disperse polymers,” *J. Polym. Sci. Polym. Phys. Ed.* **23**(1), 159–177 (1985).
- M. J. Struglinski and W. W. Graessley, “Effects of polydispersity on the linear viscoelastic properties of entangled polymers. 1. Experimental observations for binary mixtures of linear polybutadiene,” *Macromolecules* **18**(12), 2630–2643 (1985).
- S. T. Milner, T. C. B. McLeish, R. N. Young, A. Hakiki, and J. M. Johnson, “Dynamic dilution, constraint-release, and star–linear blends,” *Macromolecules* **31**(26), 9345–9353 (1998).
- Z. Wang, X. Chen, and R. G. Larson, “Comparing tube models for predicting the linear rheology of branched polymer melts,” *J. Rheol.* **54**(2), 223–260 (2010).
- M. Kapnistos, D. Vlassopoulos, J. Roovers, and L. G. Leal, “Linear rheology of architecturally complex macromolecules: Comb polymers with linear backbones,” *Macromolecules* **38**(18), 7852–7862 (2005).
- S. T. Milner and T. C. B. McLeish, “Parameter-free theory for stress relaxation in star polymer melts,” *Macromolecules* **30**(7), 2159–2166 (1997).
- C. Das, N. J. Inkson, D. J. Read, M. A. Kelmanson, and T. C. B. McLeish, “Computational linear rheology of general branch-on-branch polymers,” *J. Rheol.* **50**(2), 207–234 (2006).
- R. G. Larson, “Combinatorial rheology of branched polymer melts,” *Macromolecules* **34**(13), 4556–4571 (2001).
- E. van Ruymbeke, Y. Masubuchi, and H. Watanabe, “Effective value of the dynamic dilution exponent in bidisperse linear polymers: From 1 to 4/3,” *Macromolecules* **45**(4), 2085–2098 (2012).
- E. van Ruymbeke, E. B. Muliawan, S. G. Hatzikiriakos, T. Watanabe, A. Hirao, and D. Vlassopoulos, “Viscoelasticity and extensional rheology of model Cayley-tree polymers of different generations,” *J. Rheol.* **54**(3), 643–662 (2010).
- H. Watanabe, Y. Matsumiya, and E. van Ruymbeke, “Component relaxation times in entangled binary blends of linear chains: Reptation/CLF along partially or fully dilated tube,” *Macromolecules* **46**(23), 9296–9312 (2013).
- H. Watanabe, S. Ishida, Y. Matsumiya, and T. Inoue, “Test of full and partial tube dilation pictures in entangled blends of linear polyisoprenes,” *Macromolecules* **37**(17), 6619–6631 (2004).
- D. R. Daniels, T. C. B. McLeish, B. J. Crosby, R. N. Young, and C. M. Fernyhough, “Molecular rheology of comb polymer melts. 1. Linear viscoelastic response,” *Macromolecules* **34**(20), 7025–7033 (2001).
- W. P. Cox and E. H. Merz, “Correlation of dynamic and steady flow viscosities,” *J. Polym. Sci.* **28**(118), 619–622 (1958).

- ³⁰H. C. Booij, P. Leblans, J. Palmen, and G. Tiemersma-Thoone, "Nonlinear viscoelasticity and the Cox–Merz relations for polymeric fluids," *J. Polym. Sci. Polym. Phys. Ed.* **21**(9), 1703–1711 (1983).
- ³¹H. H. Winter, "Three views of viscoelasticity for Cox–Merz materials," *Rheol. Acta* **48**(3), 241–243 (2009).
- ³²Y. H. Shim, J. J. Griebler, and S. A. Rogers, "A reexamination of the Cox–Merz rule through the lens of recovery rheology," *J. Rheol.* **68**(3), 381–396 (2024).
- ³³J. D. J. Rathinaraj, B. Keshavarz, and G. H. McKinley, "Why the Cox–Merz rule and Gleissle mirror relation work: A quantitative analysis using the Wagner integral framework with a fractional Maxwell kernel," *Phys. Fluids* **34**(3), 033106 (2022).
- ³⁴F. Sniijkers and D. Vlassopoulos, "Appraisal of the Cox–Merz rule for well-characterized entangled linear and branched polymers," *Rheol. Acta* **53**(12), 935–946 (2014).
- ³⁵L. R. Schmidt, "A special mold and tracer technique for studying shear and extensional flows in a mold cavity during injection molding," *Polym. Eng. Sci.* **14**(11), 797–800 (1974).
- ³⁶L. A. Archer and Juliani, "Linear and nonlinear viscoelasticity of entangled multiarm (pom-pom) polymer liquids," *Macromolecules* **37**(3), 1076–1088 (2004).
- ³⁷E. van Ruymbeke, M. Kapnistos, D. Vlassopoulos, T. Huang, and D. M. Knauss, "Linear melt rheology of pom-pom polystyrenes with unentangled branches," *Macromolecules* **40**(5), 1713–1719 (2007).
- ³⁸S. Houli, H. Iatrou, N. Hadjichristidis, and D. Vlassopoulos, "Synthesis and viscoelastic properties of model dumbbell copolymers consisting of a polystyrene connector and two 32-arm star polybutadienes," *Macromolecules* **35**(17), 6592–6597 (2002).
- ³⁹J. K. Nielsen, H. K. Rasmussen, M. Denberg, K. Almdal, and O. Hassager, "Nonlinear branch-point dynamics of multiarm polystyrene," *Macromolecules* **39**(25), 8844–8853 (2006).
- ⁴⁰F. Sniijkers, D. Vlassopoulos, G. Ianniruberto, G. Marrucci, H. Lee, J. Yang, and T. Chang, "Double stress overshoot in start-up of simple shear flow of entangled comb polymers," *ACS Macro Lett.* **2**(7), 601–604 (2013).
- ⁴¹F. Sniijkers, H. Lee, T. Chang, C. Das, and D. Vlassopoulos, "Start-up shear flow of a well-characterized entangled H-polymer," *Eur. Polym. J.* **206**, 112806 (2024).
- ⁴²M.-C. Röpert, M. G. Schußmann, M. K. Esfahani, M. Wilhelm, and V. Hirschberg, "Effect of side chain length in polystyrene POM–POMs on melt rheology and solid mechanical fatigue," *Macromolecules* **55**, 5485–5495 (2022).
- ⁴³M.-C. Röpert, V. Hirschberg, M. G. Schußmann, and M. Wilhelm, "Impact of topological parameters on melt rheological properties and foamability of PS POM–POMs," *Macromolecules* **56**, 1921–1933 (2023).
- ⁴⁴V. Hirschberg, S. Lyu, and M. G. Schußmann, "Complex polymer topologies in blends: Shear and elongational rheology of linear/pom-pom polystyrene blends," *J. Rheol.* **67**(2), 403–415 (2023).
- ⁴⁵M. G. Schußmann, M. Wilhelm, and V. Hirschberg, "Predicting maximum strain hardening factor in elongational flow of branched pom-pom polymers from polymer architecture," *Nat. Commun.* **15**(1), 3545 (2024).
- ⁴⁶G. Liu, S. Cheng, H. Lee, H. Ma, H. Xu, T. Chang, R. P. Quirk, and S.-Q. Wang, "Strain hardening in startup shear of long-chain branched polymer solutions," *Phys. Rev. Lett.* **111**(6), 068302 (2013).
- ⁴⁷E. V. Menezes and W. W. Graessley, "Nonlinear rheological behavior of polymer systems for several shear-flow histories," *J. Polym. Sci. Polym. Phys. Ed.* **20**(10), 1817–1833 (1982).
- ⁴⁸T. Schweizer, "Comparing cone-partitioned plate and cone-standard plate shear rheometry of a polystyrene melt," *J. Rheol.* **47**(4), 1071–1085 (2003).
- ⁴⁹D. Auhl, J. Ramirez, A. E. Likhtman, P. Chambon, and C. Fernyhough, "Linear and nonlinear shear flow behavior of monodisperse polyisoprene melts with a large range of molecular weights," *J. Rheol.* **52**(3), 801–835 (2008).
- ⁵⁰F. Sniijkers, D. Vlassopoulos, H. Lee, J. Yang, T. Chang, P. Driva, and N. Hadjichristidis, "Start-up and relaxation of well-characterized comb polymers in simple shear," *J. Rheol.* **57**(4), 1079–1100 (2013).
- ⁵¹F. Sniijkers, K. Ratkanthwar, D. Vlassopoulos, and N. Hadjichristidis, "Viscoelasticity, nonlinear shear start-up, and relaxation of entangled star polymers," *Macromolecules* **46**(14), 5702–5713 (2013).
- ⁵²Q. Huang, S. Costanzo, C. Das, and D. Vlassopoulos, "Stress growth and relaxation of dendritically branched macromolecules in shear and uniaxial extension," *J. Rheol.* **61**(1), 35–47 (2017).
- ⁵³Y. Masubuchi, "Primitive chain network simulations for double peaks in shear stress under fast flows of bidisperse entangled polymers," [arXiv:2404.14629](https://arxiv.org/abs/2404.14629) (2024).
- ⁵⁴K. Osaki, T. Inoue, and T. Isomura, "Stress overshoot of polymer solutions at high rates of shear; Polystyrene with bimodal molecular weight distribution," *J. Polym. Sci. B Polym. Phys.* **38**(15), 2043–2050 (2000).
- ⁵⁵M. G. Schußmann, L. Kreutzer, and V. Hirschberg, "Fast and scalable synthetic route to densely grafted, branched polystyrenes and polydienes via anionic polymerization utilizing P2VP as branching point," *Macromol. Rapid Commun.* **45**(8), 2300674 (2024).
- ⁵⁶M. Röpert, A. Goecke, M. Wilhelm, and V. Hirschberg, "Threading polystyrene stars: Impact of star to POM–POM and barbwire topology on melt rheological and foaming properties," *Macromol. Chem. Phys.* **223**, 2200288 (2022).
- ⁵⁷S. Costanzo, G. Ianniruberto, G. Marrucci, and D. Vlassopoulos, "Measuring and assessing first and second normal stress differences of polymeric fluids with a modular cone-partitioned plate geometry," *Rheol. Acta* **57**(5), 363–376 (2018).
- ⁵⁸S. Costanzo, Q. Huang, G. Ianniruberto, G. Marrucci, O. Hassager, and D. Vlassopoulos, "Shear and extensional rheology of polystyrene melts and solutions with the same number of entanglements," *Macromolecules* **49**(10), 3925–3935 (2016).
- ⁵⁹V. Hirschberg, M. G. Schußmann, M.-C. Röpert, M. Wilhelm, and M. H. Wagner, "Modeling elongational viscosity and brittle fracture of 10 polystyrene pom-poms by the hierarchical molecular stress function model," *Rheol. Acta* **62**, 269–283 (2023).
- ⁶⁰M. Abbasi, L. Faust, K. Riaz, and M. Wilhelm, "Linear and extensional rheology of model branched polystyrenes: From loosely grafted combs to bottle-brushes," *Macromolecules* **50**(15), 5964–5977 (2017).
- ⁶¹M. Kempf, V. C. Barroso, and M. Wilhelm, "Anionic synthesis and rheological characterization of poly(p-methylstyrene) model comb architectures with a defined and very low degree of long chain branching," *Macromol. Rapid Commun.* **31**(24), 2140–2145 (2010).
- ⁶²M. Kempf, D. Ahirwal, M. Cziep, and M. Wilhelm, "Synthesis and linear and nonlinear melt rheology of well-defined comb architectures of PS and PpMS with a low and controlled degree of long-chain branching," *Macromolecules* **46**(12), 4978–4994 (2013).
- ⁶³L. Faust, M. Röpert, M. K. Esfahani, M. Abbasi, V. Hirschberg, and M. Wilhelm, "Comb and branch-on-branch model polystyrenes with exceptionally high strain hardening factor SHF=1000 and their impact on physical foaming," *Macromol. Chem. Phys.* **224**(1), 2200214 (2023).
- ⁶⁴L. J. Fetters, D. J. Lohse, S. T. Milner, and W. W. Graessley, "Packing length influence in linear polymer melts on the entanglement, critical, and reptation molecular weights," *Macromolecules* **32**(20), 6847–6851 (1999).
- ⁶⁵T. Schweizer, J. van Meerveld, and H. C. Öttinger, "Nonlinear shear rheology of polystyrene melt with narrow molecular weight distribution—Experiment and theory," *J. Rheol.* **48**(6), 1345–1363 (2004).
- ⁶⁶S. Costanzo, V. Ianniello, R. Pasquino, N. Grizzuti, G. Ianniruberto, and G. Marrucci, "Strain hardening of unentangled polystyrene solutions in fast shear flows," *Macromolecules* **55**(20), 9206–9219 (2022).
- ⁶⁷J. Cao and A. E. Likhtman, "Simulating startup shear of entangled polymer melts," *ACS Macro Lett.* **4**(12), 1376–1381 (2015).
- ⁶⁸S. Ravindranath and S.-Q. Wang, "Universal scaling characteristics of stress overshoot in startup shear of entangled polymer solutions," *J. Rheol.* **52**(3), 681–695 (2008).
- ⁶⁹K. S. Schweizer and S.-J. Xie, "Physics of the stress overshoot and chain stretch dynamics of entangled polymer liquids under continuous startup nonlinear shear," *ACS Macro Lett.* **7**(2), 218–222 (2018).
- ⁷⁰S. H. Jeong, J. M. Kim, and C. Baig, "Rheological influence of short-chain branching for polymeric materials under shear with variable branch density and branching architecture," *Macromolecules* **50**(11), 4491–4500 (2017).
- ⁷¹S. H. Jeong, S. Cho, and C. Baig, "Chain rotational dynamics in dilute polymer solutions and melts under shear flow," *Polymer* **281**, 126101 (2023).
- ⁷²Y. Masubuchi, G. Ianniruberto, and G. Marrucci, "Primitive chain network simulations for H-polymers under fast shear," *Soft Matter* **16**(4), 1056–1065 (2020).
- ⁷³H. Y. Song, S. J. Park, and K. Hyun, "Distinguishing between linear and star polystyrenes with unentangled arms by dynamic oscillatory shear tests," *ACS Macro Lett.* **12**, 968–973 (2023).